Natural reducing agents for electroless nanoparticle deposition: Mild synthesis of metal/carbon nanostructured microspheres

Paul Duffy,[a] *Lyndsey A. Reynolds,*[b] *Stephanie E. Sanders,*[b] *Kevin M. Metz,*[*b] *and Paula E. Colavita* [**a,c,]

a - School of Chemistry, University of Dublin Trinity College, College Green, Dublin 2, Ireland.

b - Department of Chemistry, Albion College, 611 E. Porter St., Albion MI 49224; USA.

c - Centre for Research on Adaptive Nanostructures and Nanodevices (CRANN), Trinity College Dublin, Dublin 2, Ireland.

[*] Corresponding author e-mail: colavitp@tcd.ie; kmetz@albion.edu

Abstract

Composite materials are of interest because they can potentially combine the properties of their respective components in a manner that is useful for specific applications. Here, we report on the use of coffee as a low-cost, green reductant for the room temperature formation of catalytically active, supported metal nanoparticles. Specifically, we have leveraged the reduction potential of coffee in order to grow Pd and Ag nanoparticles at the surface of porous carbon microspheres synthesized via ultraspray pyrolysis. The metal nanoparticle-on-carbon microsphere composites were characterized using scanning electron microscopy (SEM), energy dispersive X-ray spectroscopy (EDS), X-ray diffraction (XRD) and thermal gravimetric analysis (TGA). To demonstrate the catalytic activity of Pd/C and Ag/C materials, Suzuki coupling reactions and nitroaromatic reduction reactions were employed, respectively.

1. Introduction

In recent years, much work has been carried out on the synthesis of nanometallic composite materials with the objective of creating synergies between the desirable properties of metal nanoparticles and those of a solid matrix that can serve as an embedding or anchoring medium [1]. This approach has been used for decades in heterogeneous catalysis where a solid support can have the dual function of dispersing active centers and of modulating/enhancing their reactivity. Recently, there has been great interest in the use of supported noble metal nanoparticles as catalysts; for example, Pd nanoparticles find important applications as catalysts in hydrogenation and C—C bond forming reactions like Suzuki, Heck and Sonogashira coupling (see Refs.[2, 3] and references therein). Immobilization of catalytically active Pd nanoparticles at solid supports facilitates catalyst removal and reaction work up when compared to homogeneous catalysts. Therefore, much effort has recently been devoted to developing anchoring protocols for Pd nanoparticles, thus forming a composite material that preserves the original catalytic properties while improving handling and reaction work up [4-10]. Also silver nanoparticles have numerous applications, e.g. in fuel cells [11-13], optical sensors and biological applications [14-18]. However, many of these applications rely on the ability to control nanoparticle aggregation and consequent loss of function, while at the same time preserving their chemical, optical and/or catalytic properties. In order to achieve this goal, several research groups have focused on developing supported Ag nanoparticles, e.g. Ag/polysaccharide [16, 19], Ag/graphene [20] or Ag/polymer [18] nanocarrier composites, improving transport and modulating aggregation of Ag nanoparticle active centres.

The use of carbon materials for fabricating Pd and Ag supported nanoparticles offer a number of highly attractive properties for a variety of applications. Carbon provides many advantages over polymeric or inorganic supports due to its resistance to corrosion and its relatively good biocompatibility. Furthermore, the surface chemistry of carbon can be fine tuned to display different chemical groups that can for instance impart charge, regulate basicity/acidity, control wetting behaviour or prompt biological recognition. Finally, carbon supports can be designed to display a large specific surface area which can be leveraged for the delivery of large loads of nanoparticles or small molecules.

For this reason, there have recently been increased efforts aimed at developing new methodologies for the controlled deposition/embedding of metal nanoparticles at carbon scaffolds [21-23]. Porous carbon microspheres are particularly advantageous for nanoparticle support since they can leverage all of the advantages of carbon materials while displaying a high specific surface and good transport/delivery properties, as recently shown by work in our group [24]; however, their applications as nanoparticle support have remained relatively unexplored.

In this work, we report on the use of an electroless deposition approach to the synthesis of metal nanoparticle/carbon composite microspheres. Electroless deposition/plating has emerged as an effective method for controlling the size of supported metal nanoparticles (see [25] and refs. therein). Notably, Martin and co-workers carried out work on the use of electroless deposition for the decoration of membrane supports with noble metal nanostructures (nanotubules, nanowires, etc) [26]. More recently, Metz et al. have shown that these methodologies can be used to deposit Au and Pt nanoparticles at nanostructured carbon supports [27-29]. The approach typically consists of a spontaneous reduction of the metal at a surface that is activated via formation of catalytic seed particles; plating only occurs at these catalytic centres while the dispersion and size of metal nanoparticles can be, in principle, controlled by mass transport to the surface of the nanostructured solid support [30].

Electroless plating is usually considered to be environmentally unfriendly due to the use of toxic reductants, additives in plating baths and metal containing solutions. Recently Varma and co-workers reported on the use of coffee or tea as a reducing agent for green synthesis of metal nanoparticles [31, 32]. In this work we report on the use of coffee as a low-cost, green reagent for electroless deposition at room temperature. We have leveraged the reduction potential of coffee in order to grow Pd and Ag nanoparticles at the surface of porous carbon microspheres (CM) synthesized via ultraspray pyrolysis. We have characterized the structure, morphology and composition of these palladium/carbon (Pd/CM) and silver/carbon (Ag/CM) composite microspheres using a combination of Scanning Electron Microscopy (SEM) and Energy Dispersive X-ray Spectroscopy (EDS), X-ray diffraction (XRD) and thermogravimetric analysis (TGA). Finally, in order to demonstrate that the resulting electrolessly

deposited Pd^0 and Ag^0 nanoparticles display typical surface chemistry, we show that the Pd/CM and Ag/CM composites are catalytically active in Suzuki coupling and reduction reactions, respectively. Our results show that coffee can be used as a green reduction agent in surface catalyzed electroless deposition and that carbon supported nanoparticles obtained via this new methodology display good performance as heterogeneous catalysts for organic synthesis. On the light of our reactivity studies we also discuss the potential consequences of using natural extracts in the synthesis of metallic nanoparticles for catalytic applications.

2. Experimental

Materials. Tin chloride dihydrate (96%, Fisher), palladium chloride (Fisher), silver nitrate (99% Sigma), sodium borohydride (98% Sigma), sodium hydroxide (97% Sigma), dichloroacetic acid (99% Sigma), trifluoroacetic acid (TFA, 99% Sigma), ammonia (28% Romil), 4-nitrophenol (95% BDH), hydrochloric acid (37.5% Sigma), Bromotoluene (98% Aldrich), phenylboronic acid (97.0% Aldrich) sodium carbonate (99.5% Fisher), methanol (99.99% Pharmco-Aaper), tetrahydrofuran (THF, 99.9% Sigma), hexanes (99.9%, Fisher), and decaffeinated coffee (Nescafe Original decaff) were used as received.

Synthesis of carbon and metal/carbon microspheres. Carbon microspheres (CMs) were synthesized using ultrasonic spray pyrolysis as previously reported [24, 33]. Briefly, this method involves nebulising a precursor solution of dichloroacetate to generate droplets with a narrow size distribution using a 1.67 MHz piezoelectric disk (APC International, Ltd.). Droplets generated from a 1.5 M solution of sodium dichloroacetate (NaDCA) were carried into a tube furnace by a flow of Ar, where the organic precursor underwent pyrolysis at 710 °C. CMs thus produced were collected in a bubbler containing water, filtered through 0.45 μM nylon membranes and washed thoroughly using water and ethanol.

The preparation of Ag/CM composite particles consisted of three steps: (a) sensitization with tin chloride, (b) nucleation of Ag^0 at the CM surface and (c) growth of Ag^0 particles using coffee. CMs were added to 25 mL of a 0.050 M $SnCl_2$ solution in 0.070 M aqueous TFA, to a final CM concentration of 0.2400 g/L; the CM suspension was briefly sonicated and left at room temperature for 30 min to

allow for adsorption of Sn^{+2} ions at the CM surface. The suspension was then filtered and washed with water and ethanol. CMs were then placed in 10 mL of a 0.003 M $Ag(NH_3)_2^+$ solution (ammoniacal silver nitrate or Tollens' reagent), sonicated for 5 s and left for 30 min to allow for Ag^0 to nucleate at the surface. A solution of decaffeinated coffee was prepared by adding 1.0 g of coffee powder to 200 mL of water and filtered using 0.45 μM nylon membranes; 40 mL of this coffee solution were added to the 10 mL CM suspension in $Ag(NH_3)_2^+$ solution at room temperature and left to react for 5 min. The resulting Ag/CM composite particles were then washed to remove silver salts and excess nanoparticles via centrifugation/washing cycles in Millipore water and ethanol. The preparation of Pd/CM composites was carried out as for Ag/CM microparticles except for the use of an acidified 5×10^{-3} M $PdCl_2$ solution (pH 1) instead of ammoniacal silver solution. Control experiments that omitted the Sn-sensitisation step were carried out in identical manner, except for immersion of CMs into a $SnCl_2$ solution.

Reactivity studies. Nitroaromatic reduction reactions were carried out inside a UV-Vis cuvette at room temperature. A freshly prepared 0.0103 g/L dispersion of Ag/CM in a 1.0×10^{-2} M aqueous $NaBH_4$ solution was placed in a cuvette. 4-Nitrophenol was added to a final concentration of 1.0×10^{-5} M to the cuvette, which was stirred vigorously and placed inside the UV-Vis spectrometer. Spectra in the region 280-500 nm were taken at regular time intervals in order to monitor changes in 4-nitrophenol concentration.

Coupling reactions were carried out by mixing 1.0 mg of Pd/CM, 122.0 mg (1 mmol) phenylboronic acid, 171.0 mg (1mmol) 4-bromotoluene, and 116.0 mg (2 mmol) Na_2CO_3 in 20 mL of a 2:2:1 methanol : H_2O : THF solution in a sealed plastic vial. The reaction vial was agitated overnight on a mechanical shaker table at room temperature. The Pd/CM catalysts were removed by centrifugation. The reaction products were extracted with hexanes, dried with magnesium sulfate, and then put on a rotary evaporator to remove excess solvent. The dried solid product was dissolved in methanol and analyzed by Gas-Chromatography-Mass Spectrometry (GC-MS), as previously reported [34].

Characterization techniques. Scanning Electron Microscopy (SEM) was performed at an accelerating voltage of 10 keV using a Zeiss Ultra microscope equipped with an Energy Dispersive X-

ray Spectrometry (EDS) detector (Oxford Instruments). Samples were prepared by drop casting on Si wafers from dispersions of the composite powder. Elemental analysis was carried out using the commercial standardless protocol provided with the EDS detector; this approach has been shown to provide semiquantitative estimates with relative error ≤25% [35]. The specific surface area of carbon spheres was determined via Brunauer-Emmett-Teller (BET) analysis (Quantachrome Nova Station) [36]. The sample was pre-treated at 200 °C under vacuum for 24 h prior to analysis using nitrogen as the adsorbing gas. The specific surface area was calculated using a multi-point BET plot over relative pressures in the range 0.08-0.3. Thermal Gravimetric Analysis (TGA) measurements were performed using a Perkin-Elmer Pyris 1 TGA using air as a carrier gas and a heat ramp of 10 °C/min Thoroughly washed samples at least 1 mg in weight were used for TGA studies. Samples were held at 200 °C in order to desorb physisorbed water prior to initiating the measurement ramp; masses were normalised to the weight of carbon particles at 200 °C. X-ray diffraction (XRD) was carried out on a Siemens D500 diffractometer with monochromated Cu Kα radiation; pattern analysis was carried out using commercial XRD software (EVA, Bruker). Samples were prepared by supporting Metal/CM composites on nylon membranes. Raman spectroscopy was carried out using a microraman system (Renishaw 1000) equipped with a CCD detector and excitation at 457 nm. UV-Vis spectra of nitroaromatics were obtained on a Shimadzu UV- 2401PC. The Suzuki coupling reaction products were identified and quantified by gas chromatography-mass spectrometry (GS-MS) using an Agilent model 6890 gas chromatograph coupled with a model 5973 mass spectrometer. GC-MS samples were separated on a HP-5MS column, using an injection temperature of 50 °C, followed by a 10 °C ramp per minute to 250 °C with a final 4 min hold.

3. Results and Discussion

3.1 Synthesis and characterisation of Metal/CM composites

Carbon particles used in our experiments were synthesized via ultraspray pyrolysis (USP) using a protocol developed by Skrabalak et al. [33]. CMs synthesized via USP were found to be spherical in shape and contain large open pores, as shown in Fig. 1a. BET analysis showed that CMs produced from

1.5 M NaDCA solutions had a specific surface area of 473 m^2/g. The average diameter of the particles was found to be 1.8 ± 0.5 μm, as shown in the size distribution in Fig. 1b. Fig. 1c shows the Raman spectrum of CMs obtained via USP after particle washing and drying on a glass slide. The Raman spectrum is consistent with that observed for highly graphitic amorphous carbons: it displays two peaks with maxima at 1598 and 1358 cm^{-1} that we assign to the G and D bands of amorphous carbons, respectively [24, 37]. The spectrum in Fig. 1c confirms that the organic precursor salt is pyrolyzed to form a highly graphitic material.

In order to obtain metal/carbon composite microspheres, CMs underwent a two step sensitisation and activation protocol [38], as shown in Scheme 1. First, the carbon surface was sensitised in a solution of Sn^{2+} ions which undergo complexation and ion-exchange at the CM surface. A galvanic exchange was then carried out with $PdCl_4^{2-}$ and $Ag(NH_3)_2^+$ ions in solution, which have a higher reduction potential than the Sn^{4+}/Sn^{2+} redox couple [39], yielding metallic centres at the CM surface. These metallic centers can subsequently serve as sites for further reduction of the metallic salt in solution by use of a reduction agent; in this work, the reducing agent was commercial decaffeinated coffee. Fig. 2a and 2b show the result of silver and palladium reduction using coffee at CM surfaces; metallic clusters can be clearly seen in the SEM images. Varma and co-workers [31, 32] have shown that coffee solutions can be used to reduce M^{n+} to form nanoparticles; the exact identity of the reducing agent in coffee remains unclear, although it has been hypothesized that either caffeine [31] or polyphenols [32, 40] could be responsible for metal reduction. In fact, previous work has shown that other components of coffee that are unrelated to caffeine have a reduction potential sufficiently negative to spontaneously reduce $PdCl_4^{2-}$ and $Ag(NH_3)_2^+$ ions in solution [41].

Fig. 2a shows metallic silver nanoparticle aggregates obtained by this method, which were found to have sizes in the range 100-200 nm and consist of individual smaller particles approximately 25 nm in diameter. Fig. 2b shows small and well dispersed Pd^0 nanoparticles with diameters of approximately 25 nm with little or no observed aggregation. EDS analysis of silver and palladium decorated microparticles shows that they also contain tin: 70.2% and 245% for Sn/Ag and Sn/Pd (a/a%),

respectively. This is due to the sensitization process, in agreement with reported studies of sensitization/activation mechanisms [42, 43].

Control experiments that omitted a Sn sensitisation step during the synthesis, led to the formation of few large Ag aggregates up to 800 nm in diameter, most of which were found to be in suspension instead of being anchored onto the CM surface. Similarly, the omission of a Sn sensitization step during Pd deposition led to the formation of unsupported Pd nanoparticles, 20-40 nm in diameter. These control experiments indicate that Sn sensitization plays an important role in controlling surface immobilisation and size of metal nanoparticles formed at carbon microspheres.

Fig. 3a and 3b show typical XRD patterns obtained from Ag/CM and Pd/CM composite microspheres, respectively. Fig. 3a shows the characteristic (111), (200) and (220) reflections of fcc silver at 38.12°, 44.28° and 64.46°, respectively, which yielded a lattice constant of 4.086 Å, matching the literature value (JCPDS file no. 04-0783). Fig. 3b shows (111), (200) and (220) reflections centred at 40.12°, 46.66° and 68.10°, respectively, characteristic of fcc palladium; these reflections yield a lattice parameter of 3.890 Å, in good agreement with the literature value of 3.8908 Å (JCPDS file no. 05-681). XRD measurements of bare CMs showed that the carbon scaffold only contributes a broad background to the pattern. No peaks associated to tin-containing species could be detected in XRD patterns, thus suggesting that tin remaining after sensitization is mostly present in non-crystalline form. In summary, XRD results indicate that the particles deposited at the CM surface via green electroless deposition protocols contain metallic Pd and Ag particles.

In order to determine the metal loading of metal/CM composites we carried out thermal gravimetric analysis (TGA); Fig. 4 shows TGA data for bare CMs, Ag/CMs and Pd/CMs obtained in air in the range 200-900 °C. The curve for bare CMs shows that mass loss due to oxidation occurs in the range 450-650 °C with the largest mass loss rate occurring at 624 °C; in this temperature range the mass loss can be attributed to the combustion of the graphitic carbon scaffold. A residual mass of (3.0 ±2.0)% at 900 °C is due to insoluble inorganic salts/oxides formed during NaDCA pyrolysis. TGA curves obtained from Ag/CM show a maximum mass loss rate at 624 °C, in agreement to that observed in the case of bare

CMs. In the case of Pd/CM samples, the maximum mass loss rate occurs at a significantly lower temperature of 483 °C. This is in agreement with previous reports showing that Pd nanoparticles are catalytically active towards oxidation of carbon fibers and particles [44].

The residual mass obtained from Ag/CMs and Pd/CMs after oxidation at 900 °C was (30 ± 2.0)% and (36±4)%, respectively. These values are larger than those obtained from bare CMs, as expected of particles having undergone sensitization, activation and nanoparticle deposition. Since tin remains as Sn^{4+} at the surface after sensitization steps [43], we can assume that the excess residual mass consists of SnO_2 [45, 46] and Ag^0 or Pd^0 particles. Although both Ag and Pd metal form oxides when heated in air, these oxides decompose at temperatures below 900 °C [47-49], the end-point temperature in TGA curves reported in Fig. 4. Therefore, we can attribute any residual mass arising from electrolessly deposited nanoparticles to metallic Ag^0 and Pd^0 species. After correction of the residual masses in Fig. 4 for Sn content obtained from EDS results (assuming it arises from SnO_2) and for inorganic compounds resulting from NaDCA pyrolysis, the estimated Ag/C and Pd/C mass ratios are (13.5 ± 1.5)% and (7.4 ± 1.0)% w/w, respectively. Ag/C ratios are comparable to loadings achieved previously by alternative methods on other carbon scaffolds [23, 50-52]; Pd/C loadings are in the range of those found in commercial Pd/C catalysts (5-30%).

Finally, Ag/CM and Pd/CM samples show a small but noticeable mass loss in the region 285-340 °C upon oxidation, that is absent in the case of bare CMs. This result indicates that a significant amount of organic compounds remain adsorbed at the metal/CM particles after metal reduction and multiple particle washes. Possible implications of the presence of adsorbed organics are discussed in more detail in the following section.

3.2 Catalytic Activity of Metal/CM composites

The main advantage of nanoparticle synthetic strategies based on natural extracts as reductants is the environmentally benign nature of the reducing agent/s. However, a potential drawback of such an approach consists in the simultaneous presence of several natural compounds in the reductant mixture; in the case of coffee, solutions contain a complex mix of proteins, lipids, polysaccharides, small organic

molecules and inorganic compounds [53]. Many of these molecules can strongly physisorb and cap metallic nanoparticles, thus blocking surface sites and limiting their applications in areas such as catalysis or sensing. In order to demonstrate that nanoparticles synthesized via green electroless deposition using coffee display the characteristic interfacial chemistry of metallic nanoparticles, we carried out catalytic studies on Ag/CM and Pd/CM composites using two test heterogeneous reactions.

3.2.1 Reduction of 4-nitrophenol using Ag/CM composites

We investigated the activity of Ag/CM composites in the catalytic reduction of 4-nitrophenol to 4-aminophenol by sodium borohydride. The reduction rate of 4-nitrophenol is negligible in aqueous solutions of $NaBH_4$, however, it is catalysed by the presence of noble metal nanoparticles [19, 54, 55]. Fig. 5a shows time-dependent UV-Vis spectra of Ag/CM aqueous suspensions containing 1.0×10^{-2} $NaBH_4$, after injection of 4-nitrophenol; spectra have been corrected by the scattering contribution in the microsphere suspension [56]. A maximum at 400 nm is characteristic of 4-nitrophenolate ions [54, 55, 57, 58]; the peak decreased rapidly after injection into the Ag/CM : $NaBH_4$ suspension, indicating that the arylnitro group is consumed over time. The graph also shows the appearance of a peak at 290 nm, which is attributed to the formation of 4-aminophenol [54, 55, 57, 58], thus confirming that the nitroaromatic compound is reduced to its corresponding arylamine. Control experiments confirmed that no reduction takes place in the presence of $NaBH_4$ or carbon microspheres alone, but only when Ag/CM composite particles were used in suspension. These results indicate that the reduction is due to the catalytic activity of supported Ag particles and that the Ag nanoparticle surface is accessible to species in solution.

If $NaBH_4$ is in excess with respect to 4-nitrophenol then its concentration can be assumed constant and the reaction rate becomes pseudo-first-order in the concentration of 4-nitrophenol [22, 23, 54, 57-59]. Fig. 5b shows an example of a logarithmic plot of A_t/A_0 where A_t and A_0 are the absorbances at 400 nm at time t and zero, respectively. Since the absorbances at 400 nm are proportional to the concentration of 4-nitrophenol in solution then $A_t/A_0 = C_t/C_0$. An apparent rate coefficient k_{app} was calculated near time zero from linear fits of curves such as the one in Fig. 5b [54, 57-59], yielding $k_{app} = 0.0015 \pm 0.0002$ s^{-1}.

After normalization of k_{app} by the molar concentration of silver in our suspensions (1.2×10^{-5} M), we obtain a specific rate coefficient k = 122 ± 16 s^{-1} M^{-1}, which is within the range of values observed for polymer-stabilized Ag nanoparticles (~25 nm) obtained at similar $NaBH_4$ concentrations [60], albeit much lower than values originally reported by Pradhan et al. for bare Ag nanoparticles [55]. This suggests that, although we cannot exclude the presence of a partially blocking adsorbed layer, metallic surface sites at the carbon-supported Ag aggregates are highly available to catalyse heterogeneous reactions.

3.2.2 Suzuki coupling using Pd/CM composites

To demonstrate the catalytic activity of the Pd/CM composite materials synthesised using green strategies, we employed the Suzuki coupling reaction [61]. Specifically, we explored the coupling reaction between phenylboronic acid and bromotoluene, which yields methylbiphenyl as displayed in Scheme 2. This reaction, performed in triplicate, resulted in a 40 ± 10% yield of the desired product. Furthermore, the same Pd/CM particles used three times sequentially displayed no loss in catalytic activity. Control experiments using bare carbon microspheres yielded no product.

Our results are consistent with the range of previously reported catalytic activities for supported palladium nanoparticles utilized for the Suzuki reaction. For example, Kantam et al. reported yields between 10% and 90% for the coupling reaction illustrated in Scheme 1 (room temperature, varied solvents, 12 h) catalyzed by nanopalladium on a layered double hydroxide support (LDH-Pd^0) [62]. Yields in Suzuki reactions are known to be sensitive to the combination of solvents and base used [62], and also depend on the reaction temperature and type of aryl-halide used [61]. Therefore, differences between our yields and reported yields can be the result of variations in reaction conditions, the presence of adsorbed molecules at the Pd surface, or a combination of these two factors. In summary, these results suggest that our composite system has displays a performance comparable to that of previously reported supported Pd nanoparticle systems.

4. Conclusions

We have synthesized Ag/CM and Pd/CM composite particles using porous carbon microparticles as scaffolds for electroless deposition and decaffeinated coffee as a reducing agent. Our methodology shows that this mild and environmentally benign reductant can be used for the synthesis of surface supported metal nanoparticles, thus expanding its use beyond solution based nanoparticle synthesis [31, 32]. Both Ag/C and Pd/C composite microspheres were tested in order to assess their activity as heterogeneous catalysts for organic synthesis. We found that in both cases suspensions of our composite microparticles displayed the characteristic chemistry of metallic silver and palladium nanoparticles thus indicating that, after desposition at the carbon scaffold, metallic particles offer available reactive surface sites. The reaction rates observed for Suzuki coupling and nitroaromatic reduction reactions, based on calculated metal loadings, suggest that metal/CM composites reported in this work offer excellent performance compared to similar Ag and Pd supported nanoparticle systems.

Acknowledgements.

We are grateful to the Environmental Protection Agency (EPA) Ireland for financial support of this work through grant 2008-PhD-WRM-2. Acknowledgement is made to the Donors of the American Chemical Society Petroleum Research Fund for partial support of this research. This work was supported by a grant from the Hewlett Mellon Fund for Faculty Development at Albion College (Michigan, USA). The authors are also thankful to Mr. R.J. Cullen and Dr. K. Rode at TCD for assistance with instrumentation and to Dr. Clifford Harris at Albion College for his insightful suggestions.

References

[1] D. Astruc, F. Lu, J. R. Aranzaes, Angew. Chem. 44 (2005) 7852-7872.

[2] M. Lamblin, L. Nassar-Hardy, J.-C. Hierso, E. Fouquet, F.-X. Felpin, Adv. Synth. Catal. 352 (2010) 33-79.

[3] A. Balanta, C. Godard, C. Claver, Chem. Soc. Rev. 40 (2011) 4973-4985.

[4] Y. Mei, Y. Lu, F. Polzer, M. Ballauff, M. Drechsler, Chem. Mater. 19 (2007) 1062-1069.

[5] N. Karousis, G.-E. Tsotsou, F. Evangelista, P. Rudolf, N. Ragoussis, N. Tagmatarchis, J. Phys. Chem. C 112 (2008) 13463-13469.

[6] O. Dominguez-Quintero, S. Martinez, Y. Henriquez, L. D'Ornelas, H. Krentzien, J. Osuna, J. Mol. Catal. A-Chem. 197 (2003) 185-191.

[7] S. Kidambi, M. L. Bruening, Chem. Mater. 17 (2004) 301-307.

[8] G. M. Scheuermann, L. Rumi, P. Steurer, W. Bannwarth, R. Mülhaupt, J. Am. Chem. Soc. 131 (2009) 8262-8270.

[9] S. Mahouche Chergui, A. Ledebt, F. Mammeri, F. d. r. Herbst, B. Carbonnier, H. Ben Romdhane, M. Delamar, M. M. Chehimi, Langmuir 26 (2010) 16115-16121.

[10] K. Gude, R. Narayanan, J. Phys. Chem. C 115 (2011) 12716-12725.

[11] C. Coutanceau, L. Demarconnay, C. Lamy, J. M. Lèger, J. Power Sources 156 (2006) 14-19.

[12] J. R. Varcoe, R. C. T. Slade, G. L. Wright, Y. Chen, J. Phys. Chem. B 110 (2006) 21041-21049.

[13] P. Singh, D. A. Buttry, J. Phys. Chem. C 116 (2012) 10656–10663.

[14] A. J. Haes, W. P. Hall, L. Chang, W. L. Klein, R. P. Van Duyne, Nano Lett. 4 (2004) 1029-1034.

[15] A. Haes, D. Stuart, S. Nie, R. Van Duyne, J. Fluoresc. 14 (2004) 355-367.

[16] P. Sanpui, A. Chattopadhyay, S. S. Ghosh, ACS Appl. Mater. Interfaces 3 (2011) 218-228.

[17] M. Banerjee, S. Mallick, A. Paul, A. Chattopadhyay, S. S. Ghosh, Langmuir 26 (2010) 5901-5908.

[18] Y. Zhang, L. Wang, J. Tian, H. Li, Y. Luo, X. Sun, Langmuir 27 (2011) 2170-2175.

[19] A. Murugadoss, A. Chattopadhyay, Nanotechnology 19 (2008) 9.

[20] S. Bong, Y.-R. Kim, I. Kim, S. Woo, S. Uhm, J. Lee, H. Kim, Electrochem. Commun. 12 (2010) 129-131.

[21] A. Schaetz, M. Zeltner, W. J. Stark, ACS Catalysis 2 (2012) 1267-1284.

[22] S. Tang, S. Vongehr, X. Meng, J. Mater. Chem. 20 (2010) 5436-5445.

[23] P. Zhang, C. Shao, Z. Zhang, M. Zhang, J. Mu, Z. Guo, Y. Liu, Nanoscale 3 (2011) 3357-3363.

[24] P. Duffy, L. M. Magno, R. Yadav, S. Roberts, A. D. Ward, S. W. Botchway, P. E. Colavita, S. J. Quinn, J. Mater. Chem. 22 (2012) 432-439.

[25] M. R. Jones, K. D. Osberg, R. J. Macfarlane, M. R. Langille, C. A. Mirkin, Chem. Rev. 111 (2011) 3736-3827.

[26] V. P. Menon, C. R. Martin, Anal. Chem. 67 (1995) 1920-1928.

[27] K. M. Metz, P. E. Colavita, K. Y. Tse, R. J. Hamers, J. Power Sources 198 (2012) 393-401.

[28] K. M. Metz, D. Goel, R. J. Hamers, J. Phys. Chem. C 111 (2007) 7260-7265.

[29] K. M. Metz, K. Y. Tse, S. E. Baker, E. C. Landis, R. J. Hamers, Chem. Mater. 18 (2006) 5398-5400.

[30] M. De Leo, F. C. Pereira, L. M. Moretto, P. Scopece, S. Polizzi, P. Ugo, Chem. Mater. 19 (2007) 5955-5964.

[31] M. N. Nadagouda, R. S. Varma, Green Chem. 10 (2008) 859-862.

[32] M. C. Moulton, L. K. Braydich-Stolle, M. N. Nadagouda, S. Kunzelman, S. M. Hussain, R. S. Varma, Nanoscale 2 (2011) 763-770.

[33] S. E. Skrabalak, K. S. Suslick, J. Am. Chem. Soc. 128 (2006) 12642-12643.

[34] W.-J. Zhou, K.-H. Wang, J.-X. Wang, Z.-R. Gao, Tetrahedron 66 (2010) 7633-7641.

[35] D. E. Newbury, N. W. M. Ritchie, Scanning (2012) n/a-n/a.

[36] S. Brunauer, P. H. Emmett, E. Teller, J. Am. Chem. Soc. 60 (1938) 309–319.

[37] A. C. Ferrari, J. Robertson, Phys. Rev. B 61 (2000) 14095-14107.

[38] G. O. Mallory, J. B. Haydu (Eds.), Electroless Plating: Fundamentals and applications, American Electroplaters and Surface Finishers Society, Orlando, FL, 1990, p.

[39] in: D. R. Lide (Ed.) CRC Handbook of Physical Constants, CRC Press, 1998, pp. 6-177.

[40] S. K. Sivaraman, I. Elango, S. Kumar, V. Santhanam, Curr. Sci. 97 (2009) 1055-1059.

[41] J. M. Dimitric Markovic, L. M. Ignjatovic, D. A. Markovic, J. M. Baranac, J. Electroanal. Chem. 553 (2003) 177-182.

[42] L. M. Ang, T. S. A. Hor, G. Q. Xu, C. H. Tung, S. P. Zhao, J. L. S. Wang, Carbon 38 (2000) 363-372.

[43] M. Charbonnier, M. Alami, M. Romand, J. Appl. Electrochem. 28 (1998) 449-453.

[44] G. E. Shter, Y. Shindler, Y. Matatov-Meytal, G. S. Grader, M. Sheintuch, Carbon 40 (2002) 2547-2557.

[45] P. Patel, I.-S. Kim, J. Maranchi, P. Kumta, J. Power Sources 135 (2004) 273-280.

[46] P. Song, D. Wen, J. Phys. Chem. C 113 (2009) 13470-13476.

[47] J. W. Fergus, C. V. S. Mallipedi, D. L. Edwards, Compos. B Eng. 29 (1998) 51-56.

[48] G. Q. Chang, X. Meng, R. Y. Chen, X. Chen, L. Q. Chen, Z. Chen, Acta Phys.-Chim. Sin. 24 (2008) 1790-1796.

[49] H. Zhang, J. Gromek, G. Fernando, H. Marcus, S. Boorse, J. Phase Equilib. 23 (2002) 246-248.

[50] W. Yuan, G. Jiang, J. Che, X. Qi, R. Xu, M. W. Chang, Y. Chen, S. Y. Lim, J. Dai, M. B. Chan-Park, J. Phys. Chem. C 112 (2008) 18754-18759.

[51] Y. Chi, L. Zhao, Q. Yuan, X. Yan, Y. Li, N. Li, X. Li, J. Mater. Chem. 22 (2012) 13571-13577.

[52] G. Chao, L. Wenwen, J. Yi Zheng, K. Hao, Nanotechnology 17 (2006) 2882.

[53] G. Dèbry, Composition of coffee, in: Coffee and Health, John Libbey Eurotext, Paris, 1994, pp. 73-100.

[54] P. Herves, M. Perez-Lorenzo, L. M. Liz-Marzan, J. Dzubiella, Y. Lu, M. Ballauff, Chem. Soc. Rev. 41 (2012) 5577-5587.

[55] N. Pradhan, A. Pal, T. Pal, Langmuir 17 (2001) 1800-1802.

[56] A. Sassaroli, S. Fantini, Phys. Med. Biol. 49 (2004) N255-N257.

[57] K. Esumi, R. Isono, T. Yoshimura, Langmuir 20 (2003) 237-243.

[58] M. H. Rashid, T. K. Mandal, J. Phys. Chem. C 111 (2007) 16750-16760.

[59] S. Wunder, F. Polzer, Y. Lu, Y. Mei, M. Ballauff, J. Phys. Chem. C 114 (2010) 8814-8820.

[60] A. M. Signori, K. d. O. Santos, R. Eising, B. L. Albuquerque, F. C. Giacomelli, J. B. Domingos, Langmuir 26 (2010) 17772-17779.

[61] N. Miyaura, A. Suzuki, Chem. Rev. 95 (1995) 2457-2483.

[62] M. L. Kantam, M. S. Subhas, S. Roy, M. Roy, Synlett 2006 (2006) 633-635.

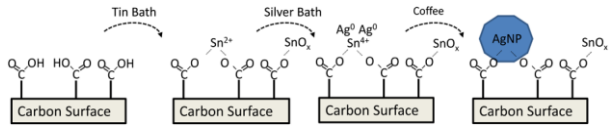

Scheme 1. Process for fabricating Ag nanoparticles anchored to carbon microsphere surfaces.

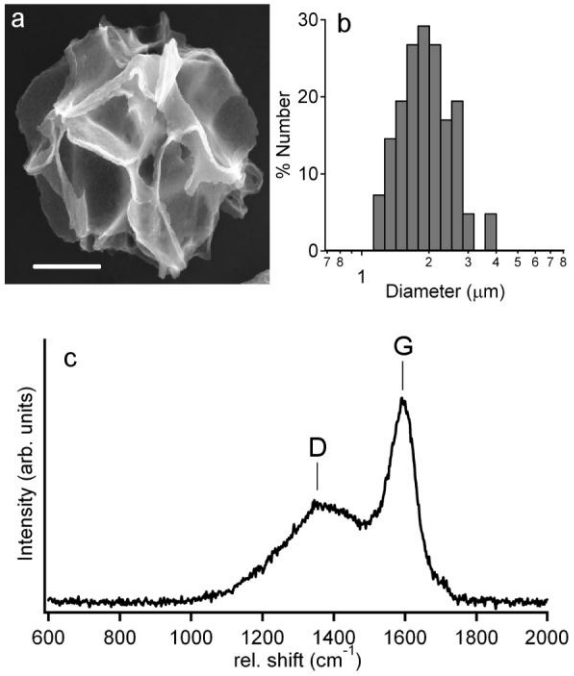

Figure 1. (a) SEM image of microspheres prepared via USP from NaDCA precursor solutions; scalebar = 500 nm. (b) Size distribution of carbon microsphere samples used in our experiments. (c) Raman spectrum of microspheres (exc. 457 nm); the profile displays the D and G bands that are characteristic of amorphous carbons.

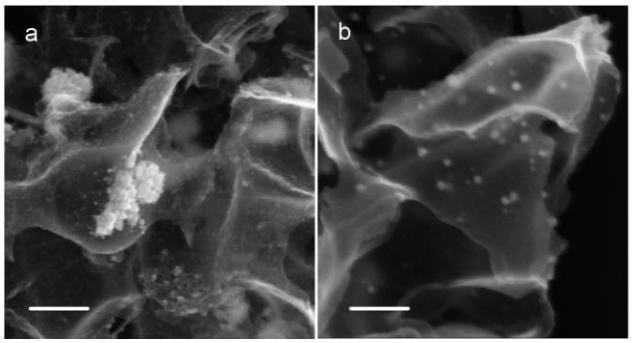

Figure 2. Typical SEM images of the Ag-decorated (a) and Pd-decorated (b) carbon microspheres obtained by using coffee as a reductant; scalebar = 200 nm.

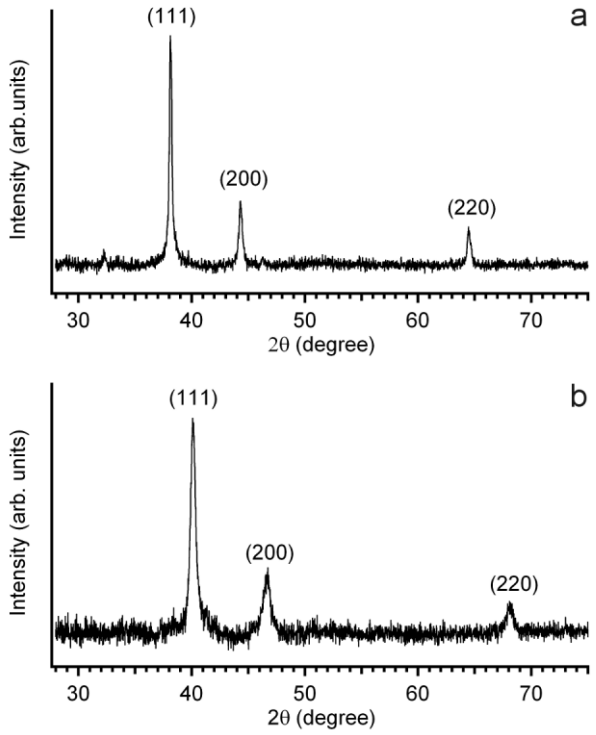

Figure 3. Powder XRD patterns obtained from Ag/CM (a) and Pd/CM (b) samples.

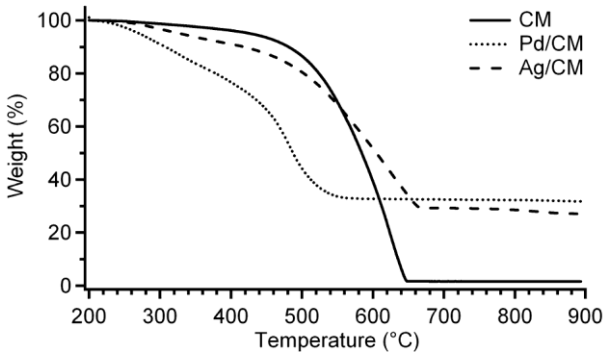

Figure 4. Thermogravimetric analysis curves (TGA) obtained in air for bare carbon microspheres (CM), Ag/CM and Pd/CM composite microspheres.

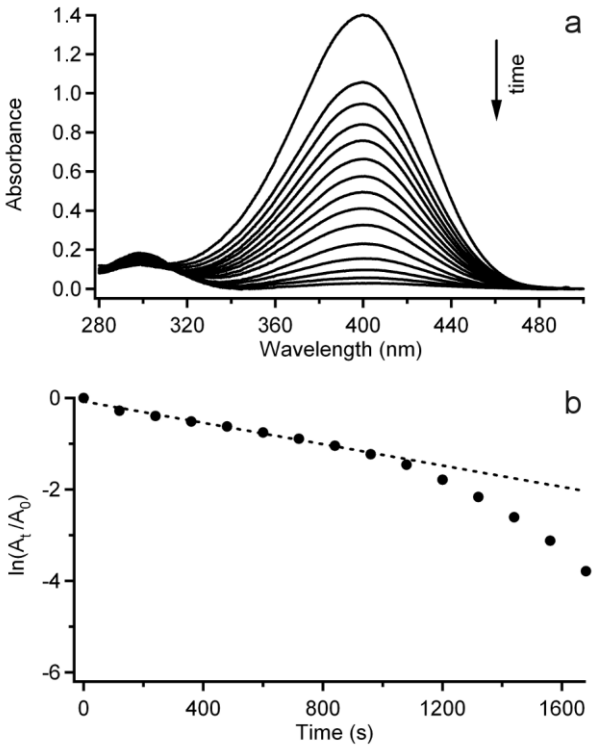

Figure 5. (a) Evolution of the UV-Vis absorption spectra of 4-nitrophenol in the presence of 1.0×10^{-2} M $NaBH_4$ and Ag/CM particles as a function of reaction time; all spectra were corrected for scattering [56]. The first spectrum was taken immediately after injection of 4-nitrophenol, whereas the last spectrum was taken after 27 min. (b) Logarithmic plot of the normalized absorbance change as a function of time. The linear fit near time zero was used to calculate the rate coefficient for the reduction reaction.

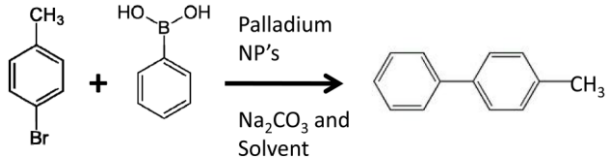

Scheme 2. The Suzuki reaction between 4-bromotoluene and phenylboronic acid, run for 18 h at room temperature. Yields of 40 ± 10% were achieved, even upon the third use of the Pd/CM catalysts.